Silk Sericin-Polylactide Protein-Polymer Conjugates as Biodegradable Amphiphilic Material and Its Application in Drug Release Systems

Kanittha Boonpavanitchakul[a], Livia K. Bast[b,c], Nico Bruns[b,c], Rathanawan Magaraphan[a,d,e]*

[a]The Petroleum and Petrochemical College, Chulalongkorn University, Phayathai, Bangkok, Thailand 10330

[b]Adolphe Merkle Institute, University of Fribourg, Chemin des Verdiers 4, CH-1700, Fribourg, Switzerland

[c]Department of Pure and Applied Chemistry, University of Strathclyde, Thomas Graham Building, 295 Cathedral Street, Glasgow G1 1XL, United Kingdom

[d]Polymer Processing and Polymer Nanomaterials Research Unit, Chulalongkorn University, Bangkok, Thailand

[e]Green Materials for Industrial Application Research Unit, Faculty of Science, Chulalongkorn University, Bangkok, 10330, Thailand

*Corresponding author: *Rathanawan.K@chula.ac.th*

Co-authors: kanittha@nanotec.or.th , livia.bast@unifr.ch, nico.bruns@strath.ac.uk

Abstract

Silk sericin (SS) is a by-product of silk production. In order to transform it into value-added products, sericin can be used as biodegradable and pH-responsive building block in drug delivery materials. To this end, amphiphilic substances were synthesized via the conjugation of hydrophobic polylactide (PLA) to the hydrophilic sericin using a *bis*-aryl hydrazone linker. PLA was esterified with terephthalaldehydic acid to obtain aromatic aldehyde terminated PLA (PLA-CHO). In addition, lysine groups of SS were modified with the linker succinimidyl-6-hydrazino-nicotinamide (S-HyNic). Then, both macromolecules were mixed to form the amphipilic protein-polymer conjugate in buffer-DMF solution. The formation of *bis*-aryl hydrazone linkages was confirmed and quantified by UV-Vis spectroscopy. SS-PLA conjugates self-assembled in water into spherical multicompartment micelles with a diameter of around 100 nm. Doxorubicin (DOX) was selected as a model drug for studying the pH-dependent drug release from SS-PLA

nanoparticles. The release rate of the encapsulated drug was slower than that of the free drug and dependent on pH; faster at pH 5.0 and resulted in a larger cumulative amount of drug released than at physiological pH of 7.4. The SS-PLA conjugate of high PLA branches showed smaller particle size and lower loading capacity than the one with low PLA branches. Both SS-PLA conjugates had negligible cytotoxicity whereas, after loading with DOX, the SS-PLA micelles were highly toxic for the human liver carcinoma immortalized cell line HepG2. Therefore the SS-based biodegradable amphiphilic material showed great potential as a drug carrier for cancer therapy.
Keywords: Silk sericin, Polylactide, Protein-polymer conjugate, Amphiphilic polymer, Drug delivery system

INTRODUCTION

Silk sericin (SS) is a water-soluble protein derived from silk cocoons by a degumming process, as a by-product of the silk textile industry. It is estimated that 100 kg of silk produces 22-30 kg of sericin protein.[1] Most SS is discarded. On the other hand, SS can become an abundantly available renewable resource. Over the past decade, many researchers attempted to develop novel biomaterials based on sericin, e.g., for wound dressing, tissue engineering, regenerative medicine, and cosmetic products.[2–5] Sericin offers many advantageous properties for biomedical applications, including being biodegradable, having high moisture absorption and low immunogenicity.[1,6–8] Moreover, sericin-based materials are not toxic and are easily metabolized within the host body.[9]

Recently, amphiphilic protein-polymer conjugates have emerged as novel materials for drug delivery applications because they can self-assemble into a wide variety of nanoscale morphologies such as micelles, nanoparticles, and vesicles.[10,11] The protein may impose stimuli-responsiveness to these structures e.g. due to protonation or deprotonation of its amino acids. Drugs can be loaded in these materials, carried into cells, and released in response to a stimulus (e.g. a drop in pH between healthy and tumor tissue). For example, amphiphilic micelles based on protein-polymer conjugates can improve the stability of hydrophobic antitumor drugs, reduce their toxicity in healthy tissues and prolong *in vivo* circulation time.[12–15] Moreover, such micelles have been designed to specifically target cancer cells.[16,17]

To synthesize amphiphilic protein-polymer conjugates based on sericin, a hydrophobic synthetic polymer has to be covalently linked to the hydrophilic protein. For example, Guo *et al.*[18]

prepared a polypeptide-based amphiphilic polymer containing sericin as the backbone and poly(γ-benzyl-*L*-glutamate) side chains via ring-opening polymerization (ROP). This product formed micelles capable of pH-triggered drug release and had low toxicity. Other kinds of SS-polymer conjugates for drug delivery applications include sericin-polyethylene glycol nanoparticles[19] and sericin-poloxamer nanoparticles.[20] A drug delivery system would ideally be composed of the protein based on sericin and a hydrophobic, biodegradable and biocompatible polymer, such as PLA.[21] However, introducing synthetic PLA onto sericin to construct a biodegradable micelle by a facile method has not been reported.

Herein, we describe the synthesis of SS-PLA conjugates by the covalent bonding of PLA to sericin using a *bis*-aryl hydrazone linker (in a buffer-DMF solution at pH 4.7 and at room temperature).[22]This linker chemistry has the additional advantage that the formed bond has a signature absorption in the UV which allows to quantify the conjugation between the protein and the polymer. The resulting SS-PLA conjugates self-assembled in aqueous solution into spherical micelle nanoparticles (i.e. multicompartment micelles) and were applied to load and release doxorubicin (DOX). The sericin protein caused the nanoparticles to be pH-responsive around its isoelectric point (pI) which is at pH 5.5-5.8.[23,24] Such acidic conditions correspond to the surroundings of tumor cells. The SS-PLA nanoparticles were thus applied as drug delivery vehicles for testing on the HepG2 cell line.

RESULTS AND DISCUSSION

Synthesis and Characterization of Silk Sericin-PLA Conjugates

Well-defined hydrophilic SS protein and hydrophobic PLA was used to synthesize an amphiphilic protein-polymer conjugate as a biodegradable material. The synthesis procedure is illustrated in Scheme 1. In the first step, PLA was synthesized via ROP of the *L*-lactide dimer with stannous octoate ($Sn(Oct)_2$) as a catalyst at 140°C.[25] In the second step, the esterification reaction between the hydroxy end group of the PLA and the carboxylic acid group of terephthalaldehydic acid lead to benzaldehyde terminated PLA (PLA-CHO), which was prepared based on a previously published method.[21,26] The ^{1}H NMR spectrum of neat PLA in $CDCl_3$ is shown in Figure 1A. The signals at 5.14 and 1.55 ppm correspond to methine (a) and methyl (b) protons of the PLA repeat unit, respectively. The signals of methine (c) and methyl (d) protons of the hydroxyl chain end unit were observed at 4.32 and 1.46 ppm, respectively, which is consistent with the literature.[27–29]

The ^{1}H NMR spectrum of PLA-CHO is shown in Figure 1B. The main characteristic peaks of PLA-CHO are the noticeable aldehyde peak at 10.09 ppm (g), and two peaks at 8.22 (f), and 7.94 (e) ppm belonging to the aromatic protons in PLA-CHO.[21] Moreover, a signal appeared at 5.38 ppm (c′) and was identified as the methine of the PLA unit next to the newly formed ester group. There is still a peak at 4.32 ppm, indicating that the esterification was not complete. The esterification efficiency was evaluated by comparing the integrals of the proton signals at 5.38 ppm (c') and 4.32 ppm (c). They are equal (Figure S1), which allows us to conclude that the esterification efficiency was 50 %.

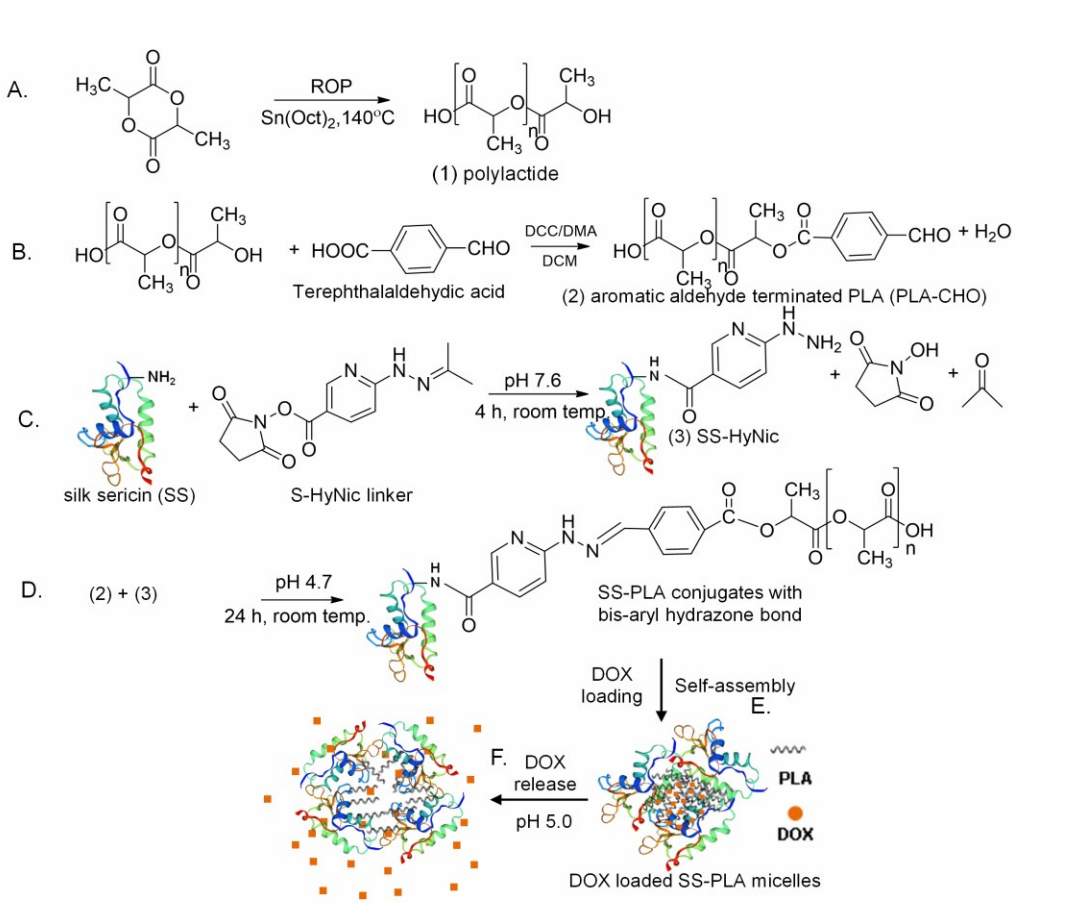

Scheme 1. Synthesis route of sericin-PLA conjugates with *bis*-aryl hydrazone bond formation. (A) Synthesis of neat PLA via ROP. (B) Synthesis of benzaldehyde-terminated PLA (PLA-CHO) via esterification. (C) Synthesis of S-HyNic labeled sericin (SS-HyNic). (D) Conjugation reaction of PLA-CHO and SS-HyNic. (E) Self-assembly of drug loaded PLA-SS micelles. (F) Drug release from micelles under pH 5.0 as a pH-responsive material.

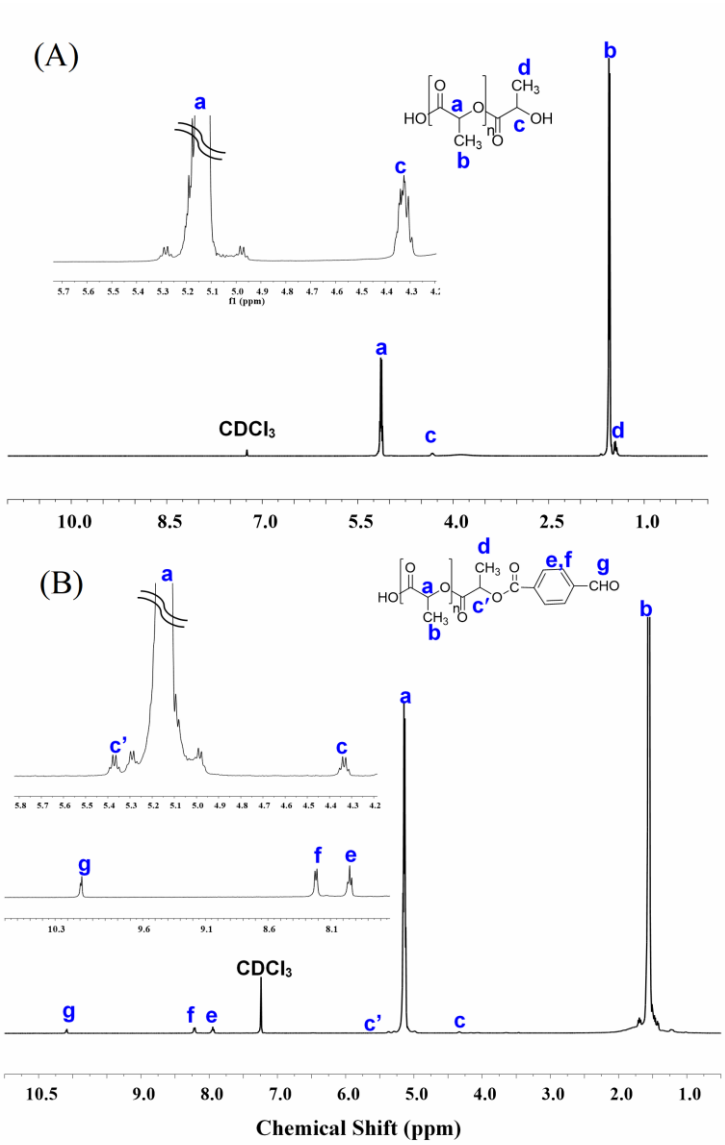

Figure 1. ^{1}H NMR spectra ($CDCl_3$, 500 MHz) of (A) PLA and (B) PLA-CHO.

According to GPC measurements, the number and weight average molecular weights (M_n) and the polydispersity index (PDI) of PLA-CHO were 11,600 kg mol^{-1} and 2.2, respectively (Table 1). The recovered yield of PLA-CHO was 80% of the employed neat PLA-

Table 1. Molecular weight (M_n, M_w) and PDI of the neat PLA and PLA-CHO

Sample	M_n[a] (g mol^{-1})	M_w/M_n[a]	Yield (%)
Neat PLA	12,300	2.02	98
PLA-CHO	11,600	2.2	80

[a]Determined by GPC calibrated based on PS standards MW 1,220-1,214,000 g mol^{-1} in THF (1.0 mL min^{-1} at 35ºC, a PLgel 10µm mixed B2 packed columns).

In the third step, lysine residues (the protein contains a total of 44 of them)[23] of silk sericin were modified with succinimidyl 6-hydrazinonicotinamid acetone hydrazone (S-HyNic) resulting in a hydrazine linker on SS (Scheme 1). The effects of varying SS concentrations (5.7, 11.4, 22.7, 37.9 µM) at constant S-HyNic concentration of 5 mM, and of varying S-HyNic concentrations (1, 3, 5, 10 mM) at constant SS concentration of 22.7 µM on the conjugation reaction were investigated. S-HyNic labeling was quantified via *bis*-aryl hydrazone bond formation with 4-nitrobenzaldehyde. This *bis*-aryl hydrazone bond has an absorbance maximum at 380 nm in UV-Vis spectra (Figure S2A and S2B) and its extinction coefficient is known.[22] The molar substitution ratio (% $MSR_{(HyNic)}$) of the S-HyNic-labeled SS were calculated according to equation 1 and are shown in Table 2. The % $MSR_{(HyNic)}$ increases with increasing SS concentrations from 5.7 µM to 22.7 µM and then remains constant. Hence, an SS concentration of 22.7 µM was used to study the effect of different concentrated S-HyNic solutions on the modification reaction. The % $MSR_{(HyNic)}$ increases with increasing concentration of the reagent, and a molar substitution ratio up to 25.8 % was achieved. The ratio of HyNic linkers per sericin molecule is a tool to design the molecular architectures of SS-PLA conjugates. For example, 7.3% $MSR_{(HyNic)}$ implies that 3 hydrazine linkers are present on average on each SS molecule. A 15.6 % $MSR_{(HyNic)}$ translates to 7 linkers per protein. As the number of linkers determines the number of polymer chains that can be attached to each protein molecule, a variety of architectures of protein-polymer conjugates can be obtained. We chose to study two different SS-HyNic values to conjugate to PLA-CHO: 7.3 % and 15.6 % (low and high % $MSR_{(HyNic)}$, respectively).

In the fourth step, the conjugation of the protein with the polymer was carried out by mixing SS-HyNic and PLA-CHO in a mixture of MES buffer and DMF (1:1) at pH 4.7 for 24 h (Scheme 1D). The solvent mixture is not harmful to the protein (as it stays in solution) and dissolves the hydrophobic PLA-CHO. SS-PLA conjugates were purified by ultra-centrifugal filters (MWCO

30 kDa) to remove any unreacted PLA. The % $MSR_{(conjugate)}$ refers to the molar ratio of hydrazone bond and sericin, which was calculated according to Lambert-Beer's law, where the experimental absorbance at 354 nm is divided by the concentration of sericin, the molar extinction coefficient of the hydrazone bond and path length (equation 2). The results are presented in Table 2. A 1:1 molar ratio of [SS-HyNic]:[PLA-CHO] resulted in an MSR of 15.0 ± 0.2 % for the final conjugate, initiated from an SS-HyNic with a MSR of 15.6. This protein-polymer conjugate will be referred to as SS-PLA high conjugation (HCJ) in the rest of the text. The conjugation of SS-HyNic 7.6 % with PLA-CHO gave a protein-polymer conjugate with a MSR of 7.8 ± 0.2 %. It will be referred to as SS-PLA low conjugation (LCJ) in the remaining text. It can be concluded that all available hydrazine linkers were modified with PLA-CHO and SS-PLA is successfully synthesized for the complete conjugation at a 1:1 molar ratio of protein and polymer. Taken together, these data suggest that sericin and PLA were well conjugated.

Table 2. Degree of modification of lysine residues on SS with S-HyNic and degree of conjugation of lysine residues on SS with PLA.

Conditions of labelling reaction			Conditions of conjugation reaction		
Concentration		% $MSR^{a}_{(HyNic)}$	Molar ratio of PLA-CHO/ SS-HyNic		% $MSR^{b}_{(Conjugate)}$
Sericin (μM)	S-HyNic (mM)		PLA-CHO	SS-HyNic (% MSR_{HyNic}=15.6%)	
5.7	5	10.8 ± 1.2	0.1	1	1.5 ± 0.2
11.4	5	12.6 ± 0.2	0.3	1	4.0 ± 0.1
22.7	5	15.6 ± 0.2	0.5	1	8.0 ± 0.4
33.9	5	16.5 ± 0.5	1	1	15.0 ± 0.2
22.7	1	7.6 ± 0.1	PLA-CHO	SS-HyNic (% MSR_{HyNic}=7.6%)	% $MSR^{b}_{(Conjugate)}$
22.7	3	10.6 ± 0.3			
22.7	5	15.6 ± 0.2			
22.7	10	25.8 ± 0.9	1	1	7.8 ± 0.2

[a] % $MSR_{(HyNic)}$ calculated by using eq.1 and absorbance at 380 nm of the UV-Vis spectra shown in Figure 2a, assuming 44 lysine molecules per molecule of sericin protein and M(SS) = 117.3 kDa.[18] [b] % $MSR_{(conjugate)}$ calculated by using eq.2 and absorbance at 354 nm of the UV-Vis spectra shown in Figure 2b and 2c (average of n=3, error = SD).

Many researchers have shown that SS may exist in different molecular weight forms, depending on the extraction process, temperature, time for processing, and acid-base conditions. [30,31] In this work, silk sericin was extracted in hot water. The procedure is thoroughly described in S2. The molecular weight of unmodified sericin and SS-PLA conjugates was determined by sodium dodecyl sulfate-polyacrylamide gel electrophoresis (SDS-PAGE). According to the SDS-PAGE results shown in Figure 2A (lane 2-3), unmodified SS is a mixture of proteins with molecular weights between 60-150 kDa. The electrophoretic pattern of SS commonly reveals a broad range of molecular weights because SS is a family of proteins with various molecular weights as reported in previous work.[8,15,32,33] As shown in Figure 2A (lane 4-5, and lane 6-7), the results of the SDS-PAGE indicate that the molecular weight distribution of SS-PLA (HCJ) and the SS-PLA (LCJ) appeared in a continuous distribution between 70–215 kDa and 70–180 kDa, respectively. The molecular weight of SS-PLA (HCJ) is higher than SS-PLA (LCJ), which corresponds to the increased number of PLA chains conjugated on each SS molecule. Moreover, the molecular weight distribution of SS-PLA conjugates is larger by approximately 10-65 kDa than the unmodified SS. Thus, the conjugation between PLA and sericin leads to an increase in the molecular weight of SS-PLA in comparison to unmodified sericin. These results serve as evidence for the successful synthesis of the conjugated SS-PLA material.

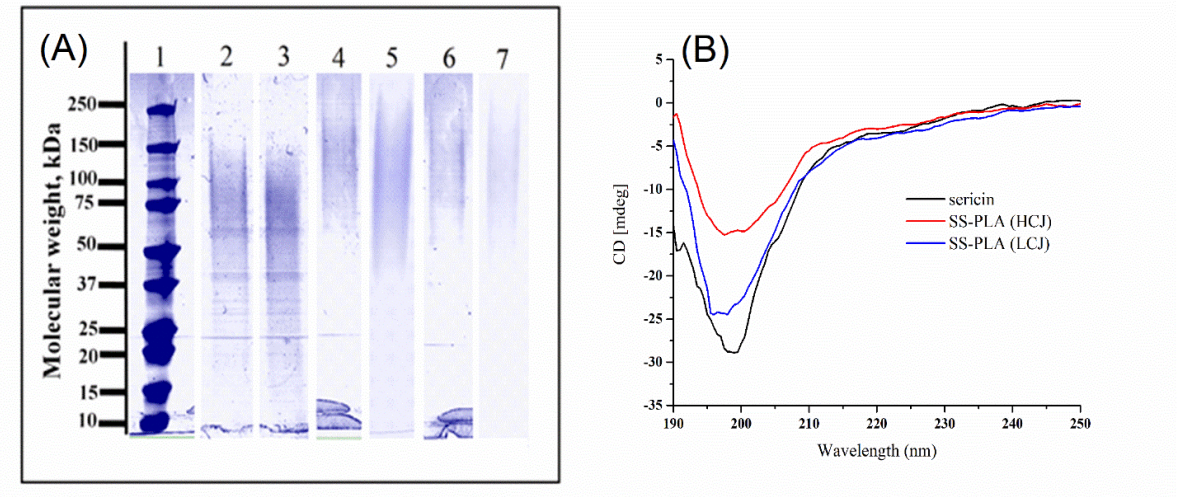

Figure 2. (A) SDS-PAGE gel of sericin (lane 2-3), SS-PLA (HCJ) (lane 4-5), and SS-PLA (LCJ) (lane 6-7), comparing with precious marker (lane 1), (B) Circular dichroism (CD) spectra of pure sericin (black line), SS-PLA (HCJ, red line), and SS-PLA (LCJ, blue line). The samples recorded with the same weight concentration.

The conformations of unmodified SS and both SS-PLA conjugate substances were investigated by circular dichroism spectroscopy (CD) (Figure 2B). For unmodified SS, the resulting spectra revealed strong and weak negative bands at 198 nm and 218 nm, which were assigned to the random coil and β-sheet conformations, respectively. These results were in accordance with previous work described by Wang *et al.*[7] and Komoto *et al.*[34] Moreover, the CD spectra of SS-PLA (HCJ) and SS-PLA (LCJ) were similar to the spectrum of unmodified sericin. It can be indicated that both SS-PLA conjugate substances maintained the ability to form random coil and β-sheet conformations. However, the CD intensities of protein after conjugation slightly differ from unmodified protein. It suggested that the high content of PLA conjugated to the sericin backbone resulted to decrease signal intensity of protein.

Self-Assembly Behavior of SS-PLA

SS-PLA conjugates are amphiphilic and should self-assemble in water into nanoscale structures such as micelles due to the hydrophobic interaction of PLA segments and the interaction of sericin with water. SS-PLA (HCJ) and SS-PLA (LCJ) self-assembled in aqueous solution (pH 7.4). Their critical micelle concentrations (CMC) were determined in the presence of pyrene using a fluorescence spectrometer. Pyrene has several vibrational bands that strongly depend on the polarity of the dye's environment.[35] The fluorescence emission spectra of pyrene in the presence of various concentrations of both SS-PLA materials are shown in Figure 3. The CMC was determined by plotting the intensity ratio of the vibrational bands at 372 nm and 382 nm for various concentrations of SS-PLA (Figure 3 inset). When the concentration reaches the CMC, the ratio of intensities I_{372}/I_{382} decreased dramatically. The CMC of SS-PLA (HCJ) and SS-PLA (LCJ) were 0.15 and 0.25 mg mL^{-1}, respectively. In other words, the CMC of SS-PLA decreased with increasing hydrophobic composition of the conjugates. In case of the SS-PLA (HCJ) material, the number of PLA chains on the sericin protein backbone is higher; therefore this conjugate is more hydrophobic than SS-PLA (LCJ).

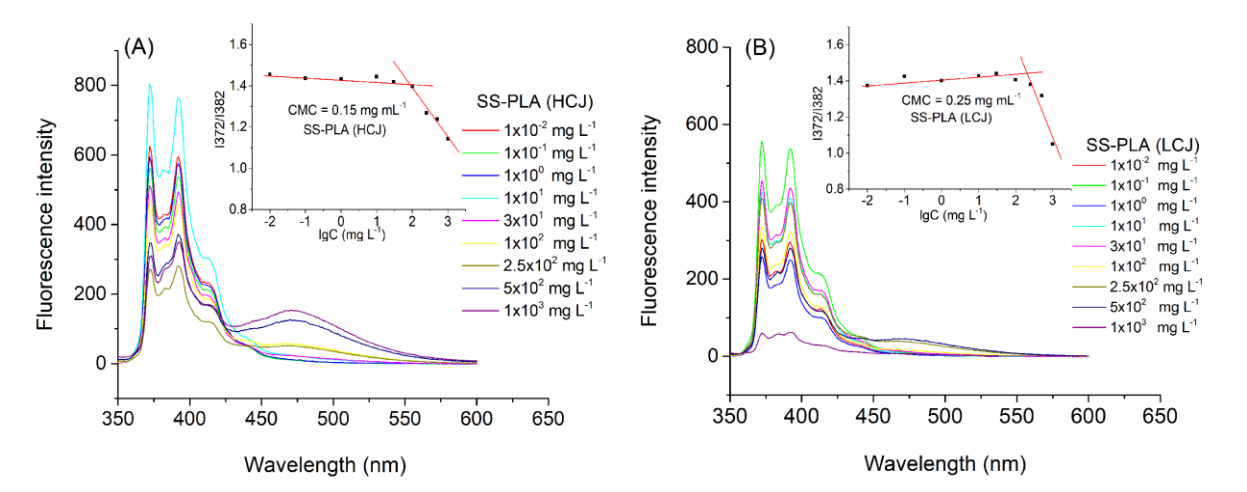

Figure 3. Pyrene encapsulation into SS-PLA self-assemblies to determine the critical micelle concentration of the protein-polymer conjugates. Fluorescence emission spectra of pyrene in water in the presence of (A) SS-PLA (HCJ), and (B) SS-PLA (LCJ); (inset) plot of the change in the intensity ratio (I_{372}/I_{382}) from excitation spectra of pyrene in water at various concentrations of SS-PLA.

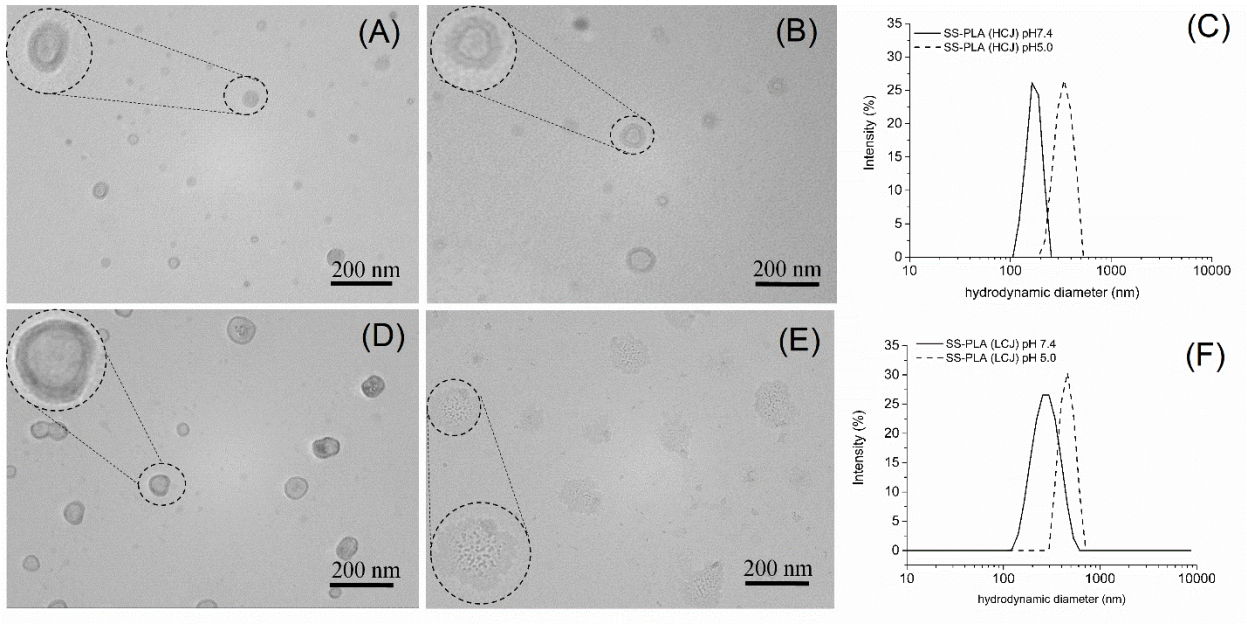

Figure 4. TEM micrographs of self-assembled structured formed by SS-PLA micelles. SS-PLA (HCJ) at (A) pH 7.4, and (B) pH 5.0; SS-PLA (LCJ) at (D) pH 7.4, and (E) pH 5.0. Hydrodynamic diameter of (C) SS-PLA (HCJ), and (F) SS-PLA (LCJ) micelles as a function of pH value.

Transition electron microscopy (TEM) provided detail information on the morphology of SS-PLA (HCJ) and SS-PLA (LCJ) self-assemblies, as shown in Figure 4. The samples were prepared in two different buffers (pH 7.4, and pH 5.0) at a higher concentration than the CMC. When SS-PLA (HCJ) and SS-PLA (LCJ) self-assembled at pH 7.4, spherical, uniform aggregates formed with a diameter 38 ± 5 nm (Figure 4A) and 76 ± 13 nm (Figure 4D), respectively. The objects appear to be solid. Their relatively large size suggests the structures are multicompartment micelles, i.e. nanoparticles composed of aggregated amphiphilic conjugates in "raspberry" morphology. Note that nothing other than the compound micelles formed. When SS-PLA (HCJ, Figure 4B) and SS-PLA (LCJ, Figure 4E) formed micelles under acidic conditions (pH 5.0), the particles size of the SS-PLA (HCJ) and SS-PLA (LCJ) micelles increased notably to 62 ± 7 nm and 142 ± 44 nm, suggesting swelling of micelles in acidic condition. Moreover, the particle size of SS-PLA (HCJ) was smaller than SS-PLA (LCJ), most likely because the hydrophobic part on SS-PLA (HCJ) led to a more compact core of the particles. In addition, the hydrodynamic diameters of micelles assembled from SS-PLA (HCJ) and SS-PLA (LCJ) were determined using Dynamic Light Scattering (DLS) as shown in Figures 4C and 4F. The self-assembled structures formed in acidic conditions (pH 5.0) were larger than those formed under neutral conditions (pH 7.4). In case of the SS-PLA (HCJ), the size changed from 139 ± 4 nm, PDI = 0.4 (pH 7.4) to 225 ± 13 nm, PDI = 0.3 (pH 5.0) and for SS-PLA (LCJ), the size changed from 260 ± 10 nm, PDI = 0.3 (pH 7.4) to 369 ± 7 nm, PDI = 0.3 (pH 5.0). It was found that the micelle size measured by TEM was smaller than the hydrodynamic size measured by DLS, which could be attributed to the loss of hydrated layer and shrunk of the SS-PLA during the drying process prior to TEM analysis.[36]

The change in hydrodynamic diameter in response to the different pH occurred because sericin contains both acidic and basic amino acids which are sensitive to pH variation.[37] When the pH of surrounding solution was lower than the protein´s pI value, SS was positively charged which induced repulsive force between conjugates. Thus, the micelle structure turned to a swollen and looser state. This pH-sensitivity indicates that the SS-PLA could be used as pH-responsive drug delivery vehicle.

Drug Loading into SS-PLA Micelles and *in vitro* Release

As a proof of concept, we investigated the drug loading efficiency (% loading) and drug entrapment efficiency (% EE) of SS-PLA (HCJ) and SS-PLA (LCJ) micelles after self-assembly. Doxorubicin hydrochloride (DOX · HCl) was selected as a model compound for chemotherapy. The efficiencies were determined by UV-Vis spectroscopy at 482 nm, which corresponds to the absorbance of the drug. Values were calculated according to equations 3 and 4. The loading efficiencies of SS-PLA (HCJ) and SS-PLA (LCJ) micelles were 1.8 ± 0.7 % and 3.0 ± 0.7 % (Table 3). The corresponding %EE values were 93.3 ± 1.6 % and 95.1 ± 0.2 %, respectively. The SS-PLA micelles took up almost all of the DOX that was added to the solution suggesting that the nonpolar DOX has good miscibility with PLA.[38] The lower loading of SS-PLA (HCJ) is probably a result of the high concentration of hydrophobic polymer chains in these micelles.

Table 3. DOX loading properties of SS-PLA nanoparticles.

Samples	Loading[a] (%)	EE[b] (%)
SS-PLA (HCJ)	1.8 ± 0.7	93.3 ± 1.6
SS-PLA (LCJ)	3.0 ± 0.7	95.1 ± 0.2

[a,b] *Determined by UV-Vis absorbance measurement according to the eq. 3 and 4, respectively. The process was carried out twice and the data are the average of two measurements.*

The pH-responsive drug release of DOX from SS-PLA (HCJ) and SS-PLA (LCJ) micelles, as well as of free DOX, was observed at 37 °C under neutral (pH 7.4) and acidic (pH 5.0) conditions, as shown in Figure 5. In the case of SS-PLA (HCJ), the initial release rate of DOX from micelles at pH 7.4 was higher than the release rate observed at pH 5.0. However, the cumulative release of DOX at pH 5.0 (approx. 40 %) was higher than at pH 7.4 (approx. 30 %) after 72 h. In the case of SS-PLA (LCJ), the initial release rate of DOX from micelles was significantly faster at pH 5.0 than at pH 7.4. The cumulative release at pH 7.4 and 5.0 was approx. 20 % and 50 %, respectively, in 72 h. Sericin is a zwitterion composed of acidic and basic amino acids with isoelectric point at pH 5.5-5.8 making it responsive to pH variation.[39,40] The drug release of DOX from SS-PLA (LCJ) nanoparticles is modulated more strongly by pH than from SS-PLA (HCJ) nanoparticles because the protein content is in SS-PLA (LCJ). Additionally, the released amount of DOX from SS-PLA micelles was time-dependent, initially increasing with time up to the equilibrium time; i.e. 20 and 30 h for SS-PLA (LCJ) and SS-PLA (HCJ), respectively. Beyond

the equilibrium time, the cumulative released amount were slightly increased or rather stable and tentatively prolonged more than 72 h.

For comparison, the release behavior of free DOX was investigated, i.e. the diffusion of free DOX across the dialysis membrane used in these experiments (Figure 5C). It was much faster and higher than the DOX release from the SS-PLA micelles at both pH 7.4 and 5.0 (cumulative release approx. 45 % and 70 %, respectively, within 12 h). The total release time of free DOX was approximately within 24 h.

To conclude, the DOX concentration released from both SS-PLA conjugates was lower than that of free DOX at the same time. Thus, the drug release test indicates that the SS-PLA micelles have the ability to prolong the release of drugs, and the SS-PLA conjugates could be feasible drug carriers to release drugs in the acidic pH conditions found in tumors. These results of nano-size morphology enhancing permeation to cell, good miscibility with DOX and good retention effect suggested that SS-PLA conjugates could be utilized as pH-responsive amphiphilic material for drug delivery purposes.

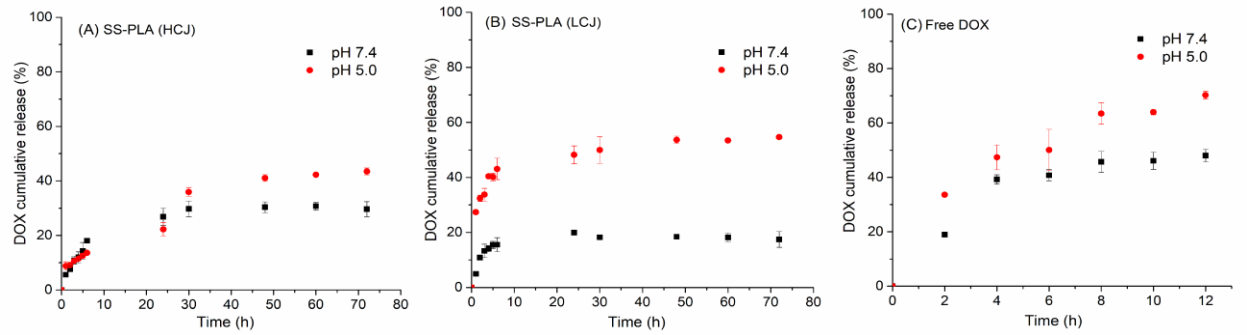

Figure 5. pH-dependent drug release from SS-PLA nanoparticles. (A) Release of DOX from SS-PLA (HCJ), (B) release of DOX from SS-PLA (LCJ), and (C) release of free DOX. pH 7.4 (phosphate buffer, black marks), pH 5.0 (acetate buffer, red marks).

***In Vitro* Cytotoxicity of SS-PLA Micelles and of DOX-loaded SS-PLA Micelles**

The cytotoxicity of SS-PLA conjugates without DOX and unmodified sericin was investigated, and the results confirmed that these materials presented low toxicity. The human liver carcinoma immortalized cell line (HepG2) was used to determine the *in vitro* cytotoxicity by the MTT assay.[15,41] The cells were exposed to a series of concentrations of SS-PLA nanoparticles (3.91 μg mL^{-1} to 1 mg mL^{-1}). As expected from the benign chemical composition of the SS-PLA conjugates, no loss of cell viability occurred, as shown in Figure 6A. These data suggest that the SS-PLA micelles could prompt negligible systemic toxicity.[38] The cytotoxicity data shown in Figure 6B were obtained from HepG2 cell line treated with a series of equivalent concentrations of DOX-loaded SS-PLA and free DOX (between 1 μg mL^{-1} to10 μg mL^{-1} DOX). The cell viability in response to DOX-loaded SS-PLA micelles decreased with increasing drug concentration and fell to 30 % at 10 μg mL^{-1} DOX. Additionally, the half maximal inhibitory concentration (IC_{50}) values of free DOX was 0.2 μg mL^{-1} for 24 h. By contrast, the IC_{50} values of the both SS-PLA conjugates were the same 6.5 μg mL^{-1} for 24 h. Within the margin of error, the cytotoxicity of DOX-loaded SS-PLA (HCJ) and SS-PLA (LCJ) were similar. Thus, the smaller size of SS-PLA (LCJ) was compensated by higher drug loading and higher release.

Free DOX was more vigorous than DOX-loaded SS-PLA micelles as it led to higher cytotoxicity. These results were in agreement to the cumulative release content in Figure 6.5, the free DOX diffused quickly into the cells while the SS-PLA micelles slowly released the drug. At high DOX concentration (10 μg mL^{-1}), not only the cytotoxicity of DOX-loaded SS-PLA nanoparticles was much improved but also the gap between cell viability between free DOX and DOX-loaded SS-PLA nanoparticles were reduced suggesting that the cytotoxicity to tumor cells from DOX-loaded SS-PLA nanoparticles became more effective. Thus the SS-PLA nanoparticles could be chosen to use for effective cytotoxicity based on relevant concentration of drug.

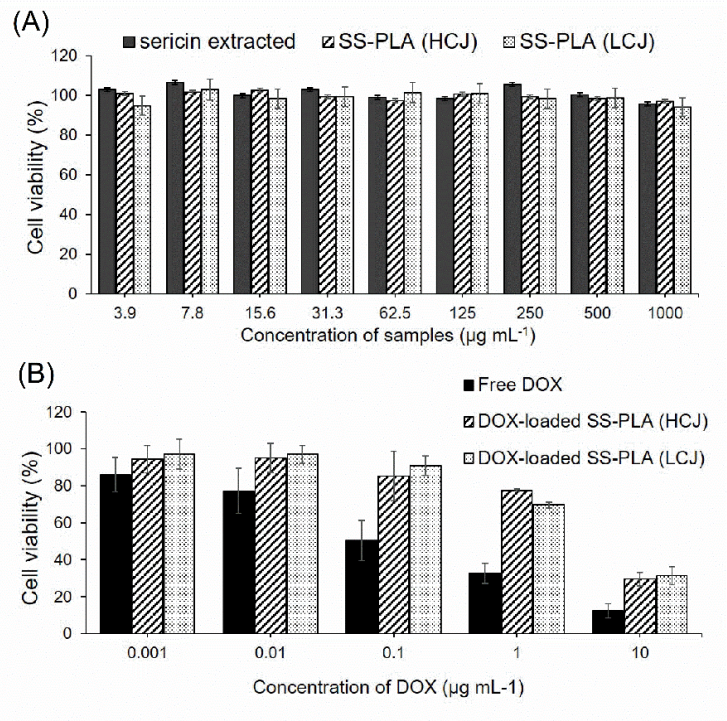

Figure 6. Viabilities of HepG2 cells treated with (A) sericin, SS-PLA (HCJ) and SS-PLA (LCJ) without DOX, (B) free DOX, DOX-loaded SS-PLA (HCJ) and SS-PLA (LCJ) after incubation for 24 h. Error bars indicate the standard deviation of three separate experiments.

Fluorescence microscopy images indicated intracellular localization of DOX from drug-loaded SS-PLA micelles and of free DOX after 6 h incubation (Figure 7). The red fluorescence of DOX was co-localized with the blue fluorescence of the DAPI stained nuclei. The DOX-loaded SS-PLA (HCJ) did not differ appreciably from the DOX-loaded SS-PLA (LCJ). It can be concluded that the SS-PLA micelles effectively delivered DOX to cells. Generally, the extracellular matrix of tumor tissue is acidic around the cells due to the lactic acid generated by acidic intracellular organelles and hypoxia.[39] Thus, the nano-sizes SS-PLA micelles swelled in response to acid environment and released the drug into the tumor cells.

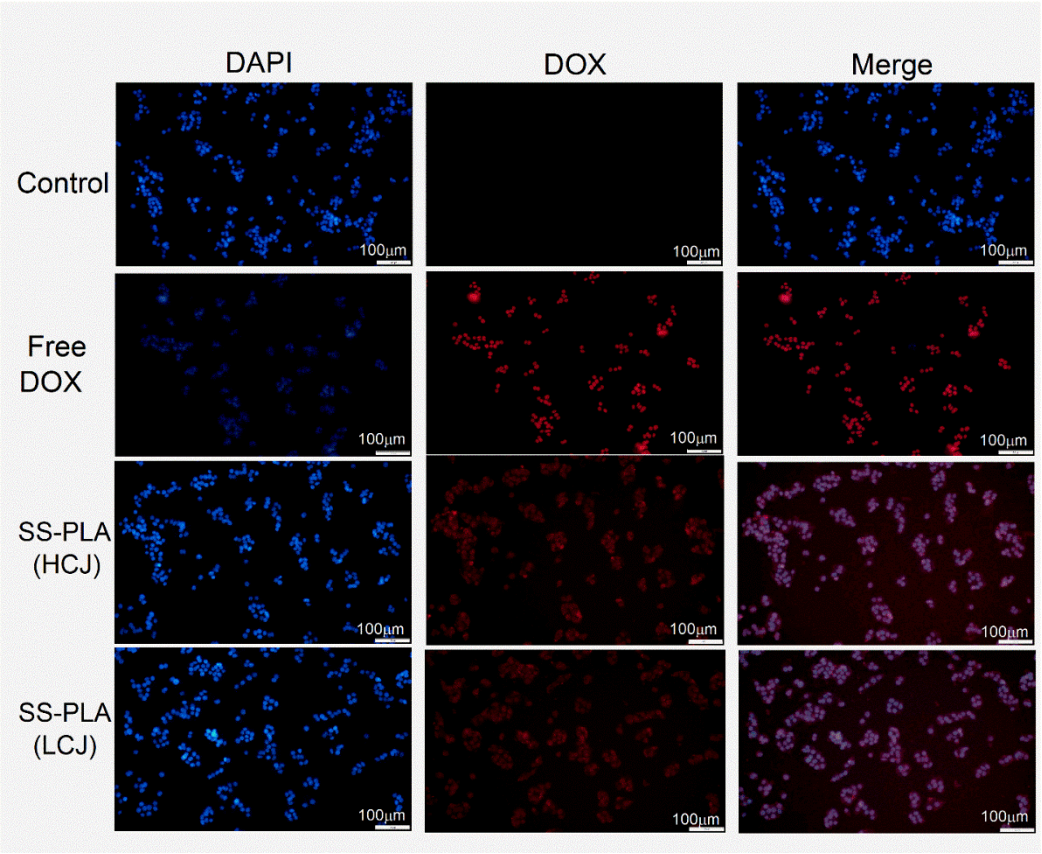

Figure 7. Fluorescence microscopy images of HepG2 cells treated free DOX and DOX-loaded SS-PLA (HCJ) and DOX-loaded SS-PLA (LCJ) at 37 °C for 6 h (DOX concentration = 10 μg mL^{-1}). Red fluorescence = DOX, Blue fluorescence = cell nuclei were stained with DAPI. Scale bar = 100μm.

CONCLUSIONS

In summary, amphiphilic SS-PLA protein-polymer conjugates were developed from the hydrophilic silk sericin and the hydrophobic biodegradable PLA. Conjugation was achieved via *bis*-aryl hydrazone bond formation under mild condition at ambient temperature to yield sericin-polymer conjugates consisting of PLA chains grafted to the sericin as proven by specific UV absorption at 380 nm. The protein did retain most of its secondary structure, as confirmed by circular dichroism spectra before and after modification. Two optimum MSR_{HyNic} on sericin were chosen at 7.6% and 15.6% and SS-HyNic moiety were reacted with PLA-CHO at 1:1 molar ratio to yield two SS-PLA types, SS-PLA (LCJ) and SS-PLA (HCJ) having MW of 100-250 kDA, as determined by SDS PAGE. The obtained SS-PLA conjugates self-assembled into multicompartment micelles of "raspberry" morphology with particle size less than 100 nm that had no cytotoxicity. These multicompartment micelles could be loaded with the drug DOX during self-assembly. SS-PLA conjugates responded to an acid environment and released more DOX in acidic condition than in neutral conditions. Moreover, SS-PLA multicompartment micelles could be used to deliver DOX to cancer cells. When loaded with DOX, both SS-PLA types had similar efficacy to kill cancer cells. In conclusion, this research did not only result in a biocompatible drug delivery system but also provided a method to make use of sericin, an industrial waste product from the silk industry.

EXPERIMENTRAL SECTION

Materials

Nang noi Thai silk cocoons (*Bombyx mori*) were purchased from local silk sericulture in Thailand. *L*-lactide (99 % purity, PURALACT®B3) was kindly provided by Purac Co. Ltd., Thailand. Tin(II) 2-ethylhexanoate ($Sn(Oct)_2$, 92.5-100 % purity) was purchased from Sigma

Aldrich Corp., USA. Terephthalaldehydic acid (> 98 %), *N,N′*-dicyclohexylcarbodiimide (DCC, > 98 %), 4-dimethylaminopyridine (DMAP, > 99 %) and doxorubicin hydrochloride (DOX · HCl) were purchased from Tokyo Chemical Industry Co., Ltd., Japan. All solvents used were analytical grade. Chloroform ($CHCl_3$), tetrahydrofuran (THF), dichloromethane (DCM), propan-2-ol (IPA), diethyl ether and dimethyl formamide (DMF) were purchased from Carlo Erba Reagents, Italy. All chemicals were used without further purification. Chloroform-d (D, 99.8%) was purchased from Cambridge Isotope Laboratories, Inc., USA. The linking reagent succinimidyl 6-hydrazinonicotinamid acetone hydrazone (S-HyNic) was purchased from Synchem UG & Co. KG, Germany. All chemicals used to prepare the phosphate buffer solutions were purchased from Sigma Aldrich, Switzerland: sodium phosphate monobasic, sodium phosphate dibasic, sodium chloride, calcium chloride, MES hydrate. Sodium acetate was purchased from Ajax Finechem, Australia, and glacial acetic acid (≥99.7%) was purchased from Duksan Pure Chemicals Co., Ltd., Korea. Both chemicals were used for preparing acetate buffer solution. Chemicals for MTT assay, a HepG2 human liver cancer cell line (from the American Type Culture Collection; ATCC) was purchased from Biomedia Corp., USA. The cells were cultured in Dulbecco's modified Eagle's medium (DMEM; Gibco; Thermo Fisher Scientific, Inc., USA). The dye for staining the cells, 4′,6-diamidino-2-phenylindole (DAPI), was purchased from Thermo Fisher Scientific, Inc., USA.

Instrumentation

^{1}H NMR spectra of PLA and PLA-CHO were obtained from a Bruker Ultrashield 500 Plus (500 MHz) instrument, using $CDCl_3$ as the solvent. The molecular weight (M_n) and polydispersity (PDI) of the polymer were determined by gel permeation chromatography (GPC), with Waters e2695 separation modules (Waters Corporation, USA), and a Model 3580 refractive index (RI) Detector (Viscotek, Malvern Panalytical Ltd., UK). Tetrahydrofuran (THF) was used as an eluent at a flow rate of 1.0 mL min^{-1}, using a PLgel 10 μm mixed B2 packed column. Polystyrene standards (M_w = 1220-1214000 g mol^{-1}, Agilent Technologies, Inc., USA) were used, and measurement was performed at 35 °C with a 100 μL injection volume and a runtime of 22 min. The labeling of SS with S-HyNic and the conjugation reaction of PLA and SS were investigated by UV-Vis spectroscopy (UV-2401PC Shimadzu Corporation, Japan). Data analysis was performed using UVProbe software, version 2.21. Spectral scans were carried out over wavelengths ranging from 200 nm to 500 nm with a speed of 2 nm s^{-1} at room temperature.

Reference spectra were taken prior to each measurement using Quartz cuvettes (YiXing ZhiCheng Materials Co. Ltd, China). The critical micelle concentration (CMC) of the self-assembled micelle system of SS-PLA conjugate materials was determined by fluorescence spectroscopy (Varian Cary Eclipse, Agilent, USA) using pyrene as a fluorescence probe. The temperature was controlled at 20 °C with a Varian Cary Single Cell Peltier Accessory. The size and size distribution of micelles were determined by a dynamic light scattering device (DLS) (Zetasizer Nano ZS instrument, Malvern instruments, UK). All samples were sonicated (Crest Ultrasonics, Malaysia) for 20 min, and then the solution samples flowed through a membrane filter (0.22 μm pore size, Millipore, Merck, USA) before detection. Afterward, the solution samples extruded (20 passes) through a 0.1 μm pore size polycarbonate filter using mini extruder kit by Avanti Polar Lipids, Inc., USA. The SS-PLA conjugate concentration was fixed at 5 mg mL^{-1} in PBS buffer. All measurements were conducted in a 1 mL quartz cuvette using a 4 mW He-Ne laser operating at a wavelength of 633 nm at 25 °C; the scattering angle was fixed to 173°. Morphologies of particles were examined in a HT7800 Hitachi transmission electron microscope (TEM, Japan) at an accelerating voltage of 100 kV. A drop of the SS-PLA sample dispersion was placed onto a carbon-coated copper grid, dried at ambient temperature. The average particle size was obtained from the sizes of 15 different particles and was measured by ImageJ software calibrated with the micron marker available in the TEM micrograph. The conformation of unmodified sericin and SS-PLA conjugate material was investigated by circular dichroism spectroscopy (CD, Jasco J-815 CD spectrometer, Japan). Spectra were measured from 300 to 180 nm, with five scans at a scanning rate of 100 nm min^{-1}; the response time constant was at 0.25 s, the bandwidth was 1 nm, and the slit width was 500 μm, using a quartz cuvette at 25 °C. A range of molecular weights of sericin and SS-PLA conjugate materials were determined using sodium dodecyl sulfate-polyacrylamide gel electrophoresis (SDS-PAGE). A 10 μL sample was mixed with an equal amount of SDS-PAGE buffer (375 mM Tris-HCl pH 6.8, 12 % SDS, 60 % glycerol, 0.03 % bromophenol blue and 600 mM dithiothreitol), then incubated at 85 °C for 10 min. The samples were loaded onto 4-15 % gradient gel (TGX™ precast gels), Bio-Rad, USA and Tris-Glycine-SDS Buffer was used as a running buffer (Bio-Rad, USA). The analysis was carried out at 200 V for 35 minutes by using a GE Healthcare Life Sciences EPS 601 power supply, Sweden. Molecular weights were estimated using precision plus protein standards marker from Bio-Rad, USA.

Synthesis of neat PLA

Neat PLA was synthesized according to the literature via ring-opening polymerization of *L*-lactide with 1.25 wt % $Sn(Oct)_2$ as a catalyst at 140 °C.[25] *L*-lactide (10 g) and $Sn(Oct)_2$ were added into a single neck round bottom flask with a stir bar. The flask was placed in an oil bath and stirred at 400 rpm under argon atmosphere. The reaction was continued for 4 h until a solid product appeared in the flask. The resulting product was dissolved in chloroform and precipitated in cold methanol twice. After that, the neat PLA was dried in an oven at 40 °C until a constant weight was achieved (yield 9.73 g, 98%). ^{1}H NMR (500 MHz, $CDCl_3$, δ in ppm): 5.14 (-CH; methine proton) and 1.55 (-CH_3; methyl protons) in the repeating unit; and 4.32 (-CH; methine proton) and 1.46 (-CH_3; methyl protons of hydroxyl-side chain end unit). The *M*n were determined by GPC to be 12,300 g mol^{-1}.

Synthesis of aromatic aldehyde terminated PLA (PLA-CHO)

PLA-CHO was synthesized by the esterification reaction, according to the literature.[21,26] First, PLA (8 g, 0.32 mmol, 1 equiv) was dissolved in 150 mL dichloromethane. Then, terephthalaldehydic acid (6 g, 3.2 mmol, 10 equiv), DCC (8.2g, 3.2 mmol, 10 equiv), and DMAP (1.2 g, 0.8 mmol, 2.5 equiv) were added and the solution was stirred for 24 h at ambient temperature. The solution mixture was filtered and the filtrate was concentrated, re-dissolved in isopropanol (80 mL), and recrystallized at 0 °C for 2 h. The crude product was collected by filtration and washed with isopropanol, diethyl ether, and methanol several times to purify the product. After purification, the obtained product was dried in an oven at 40 °C, gravimetrically (yield: 6.37 g, 80 %). The chemical structure and the molecular weight of the products were characterized by ^{1}H NMR spectroscopy and gel permeation chromatography (GPC). The following ^{1}H NMR (500 MHz, $CDCl_3$) peaks were observed (δ in ppm): 5.14 (-CH; methine proton) and 1.55 (-CH_3; methyl protons) in the repeating unit; 4.32 (-CH; methine proton) and 1.46 (-CH_3; methyl protons) for the hydroxyl-side chain end unit; 10.09 (-CHO); 8.22 and 7.94 (aromatic proton); and 5.42 (-COC*H*(CH_3)O). The M_n were determined by GPC to be 11,600 g mol^{-1}.

Preparation of buffered solutions

The following buffer solutions were prepared. Phosphate buffer saline (PB1) was prepared with 0.1 M sodium phosphate and 0.15 M NaCl (pH 7.2). Phosphate buffer (PB2) was prepared with 0.1 M sodium phosphate and 1 M NaCl (pH 7.2). MES buffer (MESB1) was prepared with 0.1 M MES hydrate and 0.15 M NaCl (pH 4.7). MES buffer (MESB2) was prepared with 0.1 M MES

hydrate (pH 5.0). Phosphate buffer solution (pH 7.4) was prepared with 75 µM sodium phosphate dibasic and 25 µM sodium phosphate monobasic. Acetate buffer (pH 5.0) was prepared with 70 µM sodium acetate and 30 µM acetic acid.

Synthesis of S-HyNic labeled sericin (SS-HyNic)

The extraction method of silk sericin is thoroughly described in S2. According to Grotzky *et al.*[22], residual lysine groups in silk sericin protein were modified with S-HyNic to form a *bis*-aryl hydrazone bond. Based on an ExPasy entry[23], under accession number P07856, silk sericin protein contains 44 lysine units and has a molecular weight of 117.3 kDa. A sericin stock solution of 10 g L^{-1} was prepared in PB2. To remove agglomerates and insoluble parts, the sericin solution was centrifuged at 1200 g for 10 min; the protein concentration of the supernatant was determined via UV-Vis spectroscopy and Lambert-Beer's law ($\varepsilon_{280\,nm}$(SS) = 131,115 cm^{-1} M^{-1}).[23] To investigate how many lysine residues in silk sericin could be labeled with S-HyNic, different molar ratios of silk sericin to S-HyNic ranging from 5.7 mM to 33.9 mM were tested. For that, certain volumes of a 62.5 µM SS stock solution (pH 7.6) and a 5 mM S-HyNic solution in anhydrous DMF was mixed at ambient temperature and stirred for 4 h. Unreacted S-HyNic was removed by centrifugal filtration using an Amicon® Ultra Centrifugal filter (MWCO 3 kDa, Merck KGaA, Germany) at 1,000 rpm for 10 min (Minispin microcentrifuge, Eppendorff®, Germany). The retentate on the membrane was washed with 0.5 mL MESB1 three times. To determine the success of the labeling reaction, SS-HyNic conjugates were characterized by UV-Vis spectroscopy using 4-nitrobenzaldehyde to induce a *bis*-aryl hydrazone bond, which gives a significant peak in the near UV at 380 nm. The protocol of Grotzky *et al.*[22] was followed. In brief, 100 µL of a 0.5 mM 4-nitrobenzaldehyde solution in anhydrous DMF and 10 µL aqueous SS-HyNic solution were briefly vortexed and incubated at 37 °C for 1 h. A reference sample was prepared by adding water instead of SS-HyNic solution. The molar substitution ratio $MSR_{(HyNic)}$ was determined by dividing the absorbance at 380 nm (*bis*-aryl hydrazone bond) by the concentration of silk sericin (in mol L^{-1}), the molar extinction coefficient (ε) at 380 nm (22,000 M^{-1} cm^{-1}), and the path length of the cuvette:

$$\%MSR_{(HyNic)} = \frac{[HyNic]}{[sericin]} = \frac{A_{380nm}}{[sericin]\cdot\varepsilon_{380nm}\cdot l} \qquad \text{equation 1}$$

Synthesis of silk sericin-polylactide conjugates (SS-PLA)

The conjugation reaction between PLA-CHO and SS-HyNic was studied in a series of molar ratios of [SS-HyNic]:[PLA-CHO] (1:0.1, 1:0.3, 1:0.5, 1:1). In brief, e.g. [SS-HyNic]:[PLA-CHO] (1:1), 500 µl of 6.3 µM SS-HyNic in MESB1 solution were mixed with 500 µl of 5.4 µM PLA-CHO solution in anhydrous DMF. The reaction was carried out at room temperature in mixture solution (pH 4.7) for 24 h. Unreacted PLA-CHO was removed by centrifugal filtration using an Amicon® Ultra Centrifugal filter (MWCO 3 kDa, Merck KGaA, Germany) at 1,000 rpm for 10 min (Minispin microcentrifuge, Eppendrof®, Germany). The retentate on the membrane was washed with 0.5 ml PB1 three times. The SS-PLA conjugate was analyzed by UV-Vis spectroscopy to determine its molar substitution ratio according to *equation 6.2*,

$$\%MSR_{(conjugate)} = \frac{[\text{hydrazone bond}]}{[\text{sericin}]} = \frac{A_{354nm}}{[\text{sericin}] \cdot \varepsilon_{354nm} \cdot l} \qquad \text{equation 2}$$

where A is the absorbance of the conjugate at 354 nm, [sericin] is the concentration of silk sericin in mol L^{-1}, ε is the molar extinction coefficient of *bis*-aryl hydrazone bond at 354 nm (29,000 M^{-1} cm^{-1})[22], and l is the path length of the cuvette in cm. The SS-PLA was lyophilized (Telstar lyoQuest HT-40, Beijer Electronics, Sweden) giving a white powder.

Measurement of critical micelle concentration

To determine the critical micelle concentration (CMC) of the SS-PLA conjugate, fluorescence spectroscopy was performed using pyrene as a hydrophobic probe to confirm the formation of the micelles self-assembled, as described previously.[35] In brief, a 10 µL aliquot of 1 mM pyrene solution in acetone was added to each vial of a series of aqueous polymer solutions (1-10 µg L^{-1}). The final concentration of pyrene in each sample solution was 2.5 µM. The mixtures were sonicated for 15 min, heated at 50 °C for 2 h, and then kept in the dark at room temperature overnight to equilibrate. Fluorescence spectra of polymer solutions were recorded at an excitation wavelength of 340 nm, and the emission spectra were monitored over a wavelength range of 350–600 nm. The ratio between the intensities of the first, at 372 nm (I_1), and the third at 382 nm (I_3), vibration bands (I_1/I_3) of the pyrene fluorescence spectrum were investigated. The CMC was evaluated after fitting the semi-log plot of the intensity ratio I_1/I_3 against the concentration.

Self-assembly of SS-PLA conjugates

For aqueous self-assembly of the SS-PLA conjugates as amphiphilic substances, sample solutions were prepared by dissolving 5 mg mL^{-1} of SS-PLA in buffer solution with difference pH values (PBS : pH 7.4, acetate buffer : pH 5.0). The solution was stirred for 12 h and sonicated for 20 min, and the solution samples were filtered using 0.22 μm filters to remove large aggregates. Afterward, the solution samples extruded (20 passes) through a 0.1 μm pore size polycarbonate filter using mini extruder kit. The morphology of micelle nanoparticles was observed by TEM and the hydrodynamic diameter by DLS.

Drug Loading into SS-PLA Micelles and *in Vitro* Release

DOX-loaded SS-PLA conjugate micelles were prepared as follows: a 3.45 mM DOX-HCl was first dissolved in DMF. The solution was stirred for 1 h in the dark. Subsequently, 50 mg of SS-PLA were dissolved in 3 mL of phosphate buffer (pH 7.4), and the resulting solution was added dropwise to DOX solution while stirring. The above dispersion was stirred further for 12 h in the dark, and the solution was sonicated (Crest Ultrasonics, Malaysia) for 20 min. Afterward, the obtained solution was loaded onto Amicon® ultra centrifugal filters (MWCO 30 kDa, Merck Millipore Ltd., Ireland) and centrifuged for 10 min at 1,000 rpm to separate untrapped DOX from the DOX-loaded particles. Then, the obtained products on membrane were washed with a solution mixture (PBS : DMF = 7.5 : 2.5) and then centrifuge again. This procedure has to be repeated at least 2 times to effectively remove non-encpasulated stuff. The DOX-loaded SS-PLA conjugate micelles were lyophilized (Christ Beta 2-8 LSCplus, Germany) and determined further. The percentage of entrapment efficiency (% EE) and loading efficiency (% loading) were determined by UV-Vis spectroscopy (Perkin-Elmer Lambda 650, USA) at an absorbance wavelength of 482 nm, which were calculated as follows:[42]

$$\%EE = \frac{\text{mass of loaded drug in micelles}}{\text{mass of initially added drug}} \times 100\% \qquad \text{equation 3}$$

$$\%Loading = \frac{\text{mass of loaded drug in micelles}}{\text{total mass of polymer and loaded drug}} \times 100\% \qquad \text{equation 4}$$

The amount of DOX loaded was determined with a pure DOX reference calibration curve. The calibration curve was established by standard DOX solutions of eight concentrations in DMF. The process of DOX release was investigated and is described as follows: 25 mg of DOX-loaded SS-PLA powder was dispersed in 2 mL of buffer solution (PBS: pH 7.4, acetate buffer: pH 5.0).

Afterward, the dispersion was placed in a tied dialysis bag (Cellu ·Tep T1, MWCO 3.5 kDa, Membrane Filtration Products, Inc., USA) against 10 mL of buffer media solutions (pH 7.4 and pH 5.0) with gentle shaking at 37 °C in an incubator shaker (THERMOLAB®-1083, GFL Germany). Drug release was investigated at dialysis times of 1, 2, 3, 4, 5, 6, 12, 24, 30, 46 and 72 h. At predetermined intervals, 1 mL of buffer solution was taken out and an equal amount of fresh buffer solution was added. The released amount of DOX was measured with a UV-Vis spectrometer at 482 nm. The above release process was carried out two times, and the two measurements were averaged. The cumulative release of DOX was calculated as follow.[43,44]

$$\text{Cumulative release (\%)} = \frac{C_n V_t + \sum_{n-1}^{n=0} C_n V_s}{x} \qquad \text{equation 5}$$

where C_n is the concentration at time t, V_t is the volume of media (V_t = 10 mL), V_s is the interval volume of media (V_s = 1 mL) and x is the initial amount of DOX. The percentage of the DOX released from the micelles was plotted against time.

***In Vitro* Cytotoxicity of SS-PLA and DOX-loaded SS-PLA conjugate materials**

The *in vitro* cytotoxicity of tested SS-PLA conjugate materials without DOX as a drug was observed using an MTT assay according to ISO 10993-5.[15,41] In this study, the HepG2 human liver cancer cell line was used for cytotoxicity experiments. A concentration of HepG2 cells was prepared at $1x10^4$ cells/well and the cells (100 µL) were added to each well in 96-well plates and then incubated at 37 °C in a humidified atmosphere of 5 % CO_2 for 24 h. The HepG2 cells were treated with bare SS-PLA micelles at various concentrations (3.91 µg $mL^{-1}$to 1 mg mL^{-1}) in Dulbecco's modified Eagle's medium (DMEM). For the case of drug loading into SS-PLA materials, the cells were treated with free DOX, DOX-loaded SS-PLA (HCJ) and (LCJ) at various concentrations (1 ng mL^{-1} to 10 µg mL^{-1}) in DMEM. The cells were incubated at 37 °C for 24 h. The solution was then removed by PBS buffer (200 µL), and the cells were incubated with an MTT assay solution (100 µL of 1 g L^{-1} of MTT) for 3 h. After that, the medium was removed and the formazan crystals formed in living cells were solubilized in 100 µL of isopropanol under shaking at 37 °C for 1 h. The relative cell viability was calculated based on the absorbance at 570 nm from the spectra with a microplate reader (SpectraMax M5, Molecular Devices, UK).

Cellular Internalization

For cellular internalization, the HepG2 cells ($2x10^4$ cells/well) were seeded in a culture media 96-well plate and incubated at 37 °C for 24 h. The cells were then treated with free DOX, DOX-loaded SS-PLA (HCJ) and (LCJ) micelles at various DOX concentrations (0.001-10 μg mL^{-1}) in DMEM and incubated at 37 °C for 6 h. Cells were washed with PBS, fixed with 4 % paraformaldehyde, and then the nucleus of the cells was stained with DAPI for 20 min. The cellular uptake of DOX was visualized by a fluorescence microscope (Olympus IX73, Japan).

ASSOCIATED CONTENT

Supporting Information

The supporting information (SI) includes ^1H NMR spectra, detailed protocol of extraction method of silk sericin protein, UV-Vis spectra.

AUTHOR INFORMATION

Corresponding author

Rattanawan Magaraphan, e-mail : *Rathanawan.K@chula.ac.th*

ORCID

Kanittha Boonpavanitchakul: 0000-0002-6518-3480

Livia K. Bast: 0000-0002-0377-4074

Nico Bruns: 0000-0001-6199-9995

Rattanawan Magaraphan : 0000-0002-9548-7960

Notes

The authors declare no competing financial interest.

ACKNOWLEDGMENTS

The authors kindly thank Prof. Dr. Supapan Seraphin, Dr. Wiyong Kangwansupamonkon and Dr. Nuttaporn Pimpha, National Nanotechnology Center (NANOTEC) for fruitful discussions. This work was supported by The Thailand Research Fund through the Royal Golden Jubilee PhD-National Science and Technology Development Agency (NSTDA) scholarship (Grant No.

PHD/0107/2559). NB and LB acknowledge funding from the European Union´s Horizon 2020 research and innovation program under the Marie-Skłodowska Curie grant agreement No 772842 (ITN Plant-inspired Materials and Surfaces – PlaMatSu). The authors thank Chulalongkorn University, National Nanotechnology Center (NANOTEC), Thailand and Adolphe Merkle Institute, University of Fribourg, Switzerland for their support of the facilities and instruments. We also thank Prof. Tirayut Vilaivan, Department of Chemistry, Chulalongkorn University for use of the circular dichroism (CD) spectroscopy instrument and Dr. Sittiruk Roytrakul from the National Center for Genetic Engineering and Biotechnology (BIOTEC) for the SDS-PAGE equipment.

REFERENCES

(1) Vaithanomsat, P.; Kitpreechavanich, V. Sericin Separation from Silk Degumming Wastewater. *Sep. Purif. Technol.* **2008**, *59* (2), 129–133.

(2) Lamboni, L.; Gauthier, M.; Yang, G.; Wang, Q. Silk Sericin: A Versatile Material for Tissue Engineering and Drug Delivery. *Biotechnol. Adv.* **2015**, *33* (8), 1855–1867.

(3) Hardy, J. G.; Römer, L. M.; Scheibel, T. R. Polymeric Materials Based on Silk Proteins. *Polymer (Guildf).* **2008**, *49* (20), 4309–4327.

(4) Zhang, Y. Q. Applications of Natural Silk Protein Sericin in Biomaterials. *Biotechnol. Adv.* **2002**, *20* (2), 91–100.

(5) Kundu, S. C.; Dash, B. C.; Dash, R.; Kaplan, D. L. Natural Protective Glue Protein, Sericin Bioengineered by Silkworms: Potential for Biomedical and Biotechnological Applications. *Prog. Polym. Sci.* **2008**, *33* (10), 998–1012.

(6) Fabiani, C.; Pizzichini, M.; Spadoni, M.; Zeddita, G. Treatment of Waste Water from Silk Degumming Processes for Protein Recovery and Water Reuse. *Desalination* **1996**, *105* (1–2), 1–9.

(7) Wu, J. H.; Wang, Z.; Xu, S. Y. Preparation and Characterization of Sericin Powder Extracted from Silk Industry Wastewater. *Food Chem.* **2007**, *103* (4), 1255–1262.

(8) Gupta, D.; Agrawal, A.; Rangi, A. Extraction and Characterization of Silk Sericin. *Indian J. Fibre Text. Res.* **2014**, *39*, 364–372.

(9) Jain, A.; Singh, S. K.; Arya, S. K.; Kundu, S. C.; Kapoor, S. Protein Nanoparticles: Promising Platforms for Drug Delivery Applications. *ACS Biomater. Sci. Eng.* **2018**, *4* (12), 3939–3961.

(10) Han, G.; Wang, J.-T.; Ji, X.; Liu, L.; Zhao, H. Nanoscale Proteinosomes Fabricated by Self-Assembly of a Supramolecular Protein–Polymer Conjugate. *Bioconjug. Chem.* **2017**, *28* (2), 636–641.

(11) Liu, X.; Gao, W. In Situ Growth of Self-Assembled Protein–Polymer Nanovesicles for Enhanced Intracellular Protein Delivery. *ACS Appl. Mater. & Interfaces* **2017**, *9* (3), 2023–2028.

(12) Xu, H.; Yao, Q.; Cai, C.; Gou, J.; Zhang, Y.; Zhong, H.; Tang, X. Amphiphilic Poly(Amino Acid) Based Micelles Applied to Drug Delivery: The in Vitro and in Vivo Challenges and the Corresponding Potential Strategies. *J. Control. Release* **2015**, *199* (December), 84–97.

(13) Klok, H. A. Peptide/Protein-Synthetic Polymer Conjugates: Quo Vadis. *Macromolecules* **2009**, *42* (21), 7990–8000.

(14) Pelegri-Oday, E. M.; Lin, E. W.; Maynard, H. D. Therapeutic Protein-Polymer Conjugates: Advancing beyond Pegylation. *J. Am. Chem. Soc.* **2014**, *136* (41), 14323–14332.

(15) Minta, M.; Radko, L.; Stypua-Trebas, S.; Zmudzki, J. Cytotoxic Effects of the Synthetic Oestrogens and Androgens on Balb/c 3T3 and HepG2 Cells. *Bull. Vet. Inst. Pulawy* **2014**, *58* (4), 613–620.

(16) Li, J.; Zhang, L.; Lin, Y.; Xiao, H.; Zuo, M.; Cheng, D.; Shuai, X. A PH-Sensitive Prodrug Micelle Self-Assembled from Multi-Doxorubicin-Tailed Polyethylene Glycol for Cancer Therapy. *RSC Adv.* **2016**, *6* (11), 9160–9163.

(17) Feng, H.; Chu, D.; Li, Z.; Guo, Z.; Jin, L.; Fan, B.; Zhang, J.; Li, J. A DOX-Loaded Polymer Micelle for Effectively Inhibiting Cancer Cells. *RSC Adv.* **2018**, *8* (46), 25949–25954.

(18) Guo, W.; Deng, L.; Yu, J.; Chen, Z.; Woo, Y.; Liu, H.; Li, T.; Lin, T.; Chen, H.; Zhao, M.; et al. Sericin Nanomicelles with Enhanced Cellular Uptake and pH-Triggered Release of Doxorubicin Reverse Cancer Drug Resistance. *Drug Deliv.* **2018**, *25* (1), 1103–1116.

(19) Cho, K.; Moon, J.; Lee, K.; Yeo, J.; Kweon, H.; Kim, Y.; Cho, C. Preparation of Self-Assembled Silk Sericin Nanoparticles. *Int. J. Biol. Macromol.* **2003**, *32*, 36–42.

(20) Mandal, B. B.; Kundu, S. C. Self-Assembled Silk Sericin/Poloxamer Nanoparticles as Nanocarriers of Hydrophobic and Hydrophilic Drugs for Targeted Delivery. *Nanotechnology* **2009**, *20* (35), 355101.

(21) Cao, Y.; Zhao, J.; Zhang, Y.; Liu, J.; Liu, J.; Dong, A.; Deng, L. PH/Redox Dual-Sensitive Nanoparticles Based on the PCL/PEG Triblock Copolymer for Enhanced Intracellular Doxorubicin Release. *RSC Adv.* **2015**, *5* (36), 28060–28069.

(22) Grotzky, A.; Manaka, Y.; Kojima, T.; Walde, P. Preparation of Catalytically Active, Covalent α-Polylysine-Enzyme Conjugates via UV/Vis-Quantifiable Bis-Aryl Hydrazone Bond Formation. *Biomacromolecules* **2011**, *12* (1), 134–144.

(23) Artimo, P.; Jonnalagedda, M.; Arnold, K.; Baratin, D.; Csardi, G.; De Castro, E.; Duvaud, S.; Flegel, V.; Fortier, A.; Gasteiger, E.; et al. ExPASy: SIB Bioinformatics Resource Portal. *Nucleic Acids Res.* **2012**, *40* (W1), 597–603.

(24) Castrillón, D.; Vélez, L.; Hincapié, G.; Álvarez, C. Characterization of Colombian Silk Sericin Dehydrated by Spray Drying and Freeze Drying Characterization of Colombian Silk Sericin Dehydrated by Spray. *Adv. J. Food Sci. Technol.* **2018**, *15* (July), 5–14.

(25) Boonpavanitchakul, K.; Jarussophon, S.; Pimpha, N.; Kangwansupamonkon, W.; Magaraphan, R. Silk Sericin as a Bio-Initiator for Grafting from Synthesis of Polylactide via Ring-Opening Polymerization. *Eur. Polym. J.* **2019**, *121*, 109265.

(26) Gu, J.; Cheng, W.-P.; Liu, J.; Lo, S.-Y.; Smith, D.; Qu, X.; Yang, Z. PH-Triggered Reversible Stealth Polycationic Micelles. *Biomacromolecules* **2008**, *9* (1), 255–262.

(27) Chumeka, W.; Pasetto, P.; Pilard, J. F.; Tanrattanakul, V. Bio-Based Triblock Copolymers from Natural Rubber and Poly(Lactic Acid): Synthesis and Application in Polymer Blending. *Polymer (Guildf).* **2014**, *55* (17), 4478–4487.

(28) Chen, H. Y.; Zhang, J.; Lin, C. C.; Reibenspies, J. H.; Miller, S. A. Efficient and Controlled Polymerization of Lactide under Mild Conditions with a Sodium-Based Catalyst. *Green Chem.* **2007**, *9* (10), 1038–1040.

(29) Alba, A.; Du Boullay, O. T.; Martin-Vaca, B.; Bourissou, D. Direct Ring-Opening of Lactide with Amines: Application to the Organo-Catalyzed Preparation of Amide End-Capped PLA and to the Removal of Residual Lactide from PLA Samples. *Polym. Chem.* **2015**, *6* (6), 989–997.

(30) Hyon, S.-H.; Jamshidi, K.; Ikada, Y. Synthesis of Polylactides with Different Molecular Weights. *Biomaterials* **1997**, *18* (22), 1503–1508.

(31) Suwannaphan, S.; Fufeungsombut, E.; Promboon, A.; Chim-anage, P. A Serine Protease from Newly Isolated Bacillus Sp. for Efficient Silk Degumming, Sericin Degrading and Colour Bleaching Activities. *Int. Biodeterior. Biodegradation* **2017**, *117*, 141–149.

(32) Chirila, T.; Suzuki, S.; Bray, L.; Barnett, N.; Harkin, D. Evaluation of Silk Sericin as a Biomaterial: In Vitro Growth of Human Corneal Limbal Epithelial Cells on Bombyx Mori Sericin Membranes. *Prog. Biomater.* **2013**, *2*.

(33) Kumar, J. P.; Bhardwaj, N.; Mandal, B. B. Cross-Linked Silk Sericin–Gelatin 2D and 3D Matrices for Prospective Tissue Engineering Applications. *RSC Adv.* **2016**, *6* (107), 105125–105136.

(34) Tsukada, M.; Komoto, T.; Kawai, T. Conformation of Liquid Silk Sericin. *Polym. J.* **1979**, *11* (6), 503–505.

(35) Woraphatphadung, T.; Sajomsang, W.; Gonil, P.; Treetong, A.; Akkaramongkolporn, P.; Ngawhirunpat, T.; Opanasopit, P. PH-Responsive Polymeric Micelles Based on Amphiphilic Chitosan Derivatives: Effect of Hydrophobic Cores on Oral Meloxicam Delivery. *Int. J. Pharm.* **2016**, *497* (1–2), 150–160.

(36) Zhou, X. X.; Jin, L.; Qi, R. Q.; Ma, T. pH-Responsive Polymeric Micelles Self-Assembled from Amphiphilic Copolymer Modified with Lipid Used as Doxorubicin Delivery Carriers. *R. Soc. Open Sci.* **2018**, *5* (3).

(37) Hu, D.; Xu, Z.; Hu, Z.; Hu, B.; Yang, M.; Zhu, L. pH-Triggered Charge-Reversal Silk Sericin-Based Nanoparticles for Enhanced Cellular Uptake and Doxorubicin Delivery. *ACS Sustain. Chem. Eng.* **2017**, *5* (2), 1638–1647.

(38) Zheng, W.; Li, M.; Lin, Y.; Zhan, X. Encapsulation of Verapamil and Doxorubicin by MPEG-PLA to Reverse Drug Resistance in Ovarian Cancer. *Biomed. Pharmacother.* **2018**, *108*, 565–573.

(39) Das, S. K.; Dey, T.; Kundu, S. C. Fabrication of Sericin Nanoparticles for Controlled Gene

Delivery. *RSC Adv.* **2014**, *4* (5), 2137–2142.

(40) Chirila, T. V; Suzuki, S.; McKirdy, N. C. Further Development of Silk Sericin as a Biomaterial: Comparative Investigation of the Procedures for Its Isolation from Bombyx Mori Silk Cocoons. *Prog. Biomater.* **2016**, *5* (2), 135–145.

(41) International Organization for Standardization. Biological Evaluation of Medical Devices Part 5: Tests for in Vitro Cytotoxicity. In ISO 10993-5. In *ISO*; Geneva, Switzerland, 2009.

(42) Calik, F.; Degirmenci, A.; Eceoglu, M.; Sanyal, A.; Sanyal, R. Dendron–Polymer Conjugate Based Cross-Linked Micelles: A Robust and Versatile Nanosystem for Targeted Delivery. *Bioconjug. Chem.* **2019**, *30* (4), 1087–1097.

(43) Zhang, L.; Feng, Y.; Tian, H.; Shi, C.; Zhao, M.; Guo, J. Controlled Release of Doxorubicin from Amphiphilic Depsipeptide-PDO-PEG- Based Copolymer Nanosized Microspheres. *React. Funct. Polym.* **2013**, *73* (9), 1281–1289.

(44) Phunpee, S.; Saesoo, S.; Sramala, I.; Jarussophon, S.; Sajomsang, W.; Puttipipatkhajorn, S.; Soottitantawat, A.; Ruktanonchai, U. R. A Comparison of Eugenol and Menthol on Encapsulation Characteristics with Water-Soluble Quaternized β-Cyclodextrin Grafted Chitosan. *Int. J. Biol. Macromol.* **2016**, *84*, 472–480.